Solution Photochemistry of $(\eta^5\text{-}C_5R_5)Rh(CO)_2$ (R = H, Me) Complexes: Pathways for Photosubstitution and C-H/Si-H Bond Activation Reactions

Denis P. Drolet and Alistair J. Lees*

Contribution from the Department of Chemistry, University Center at Binghamton, State University of New York, Binghamton, New York 13902-6000. *Received August 29, 1991. Revised Manuscript Received January 28, 1992*

Abstract: The detailed ligand photosubstitution chemistry of $CpRh(CO)_2$ and $Cp^*Rh(CO)_2$ ($Cp = \eta^5\text{-}C_5H_5$; $Cp^* = \eta^5\text{-}C_5R_5$) has been investigated in deoxygenated decalin solutions containing a series of phosphine and phosphite (PR_3) ligands. The solution photoreactions have been monitored by diode-array UV-visible and FTIR spectroscopy following excitation at 313 and 458 nm. Spectral sequences recorded over the time of photolysis reveal that these photoreactions involve clean and complete conversions to the corresponding $CpRh(CO)PR_3$ and $Cp^*Rh(CO)PR_3$ products. The reactions are attributed to occur from ligand field (LF) excited states. Photochemical quantum efficiencies have been determined and in each system they exhibit a linear relationship with the entering PR_3 ligand concentration and a dependence on the nature of the scavenging nucleophile; these observations illustrate that the ligand photosubstitution reactions proceed via an associative mechanism. A comparison of the quantum efficiency results obtained for the Cp and Cp* systems indicates that the nature of the cyclopentadienyl ring substantially affects the reaction efficiency, and it is suggested that the primary photoproduct involved is formed as a consequence of a $\eta^5 \rightarrow \eta^3$ ring slip process. The photochemistry of $CpRh(CO)_2$ and $Cp^*Rh(CO)_2$ has also been studied in triethylsilane (Et_3SiH) solution to determine the nature of the Si-H bond activation reaction. In these cases the observed quantum efficiency values are independent of Et_3SiH concentration, illustrating that these reactions proceed via a CO dissociative process. Ligand photosubstitution quantum efficiencies obtained following 313-nm excitation provide further evidence for the participation of the dissociative mechanism arising from a higher energy LF excited state. The experimental results lead to a postulated mechanistic scheme that represents both the ligand photosubstitution and photochemical C-H/Si-H bond activation pathways and to a description of the reaction intermediates involved.

Introduction

An exciting development in organometallic chemistry in recent years has been the use of transition-metal complexes to activate the normally unreactive C-H bonds of saturated carbon centers under relatively mild homogeneous conditions.[1] In this regard there is a renewed interest in the photochemistry of $(\eta^5\text{-}C_5R_5)ML_2$ and $(\eta^5\text{-}C_5R_5)ML(H)_2$ (M = Rh, Ir; L = CO, olefin, PR_3) complexes[2] following the discovery that these reactions generate photoproducts deriving from their intermolecular insertion into the C-H bonds of unactivated hydrocarbon molecules.[3,4] One of the most important questions raised by these studies concerns the identity and reactivity of the primary photoproducts that are generated. Several experimental approaches have been adopted to tackle this problem; these include extensive synthetic and kinetic investigations[4,5] and the employment of various photochemical techniques, such as matrix isolation,[6,7] flash photolysis,[8] and low-temperature studies that incorporate liquefied noble gases as inert solvents.[9] The results obtained from these studies suggest that both ligand substitution and C-H bond activation photoreactions take place via 16-electron coordinatively-unsaturated intermediates of the general formula $(\eta^5\text{-}C_5R_5)ML$, although it should be pointed out that these species are clearly extremely reactive and have only been observed spectroscopically in trace amounts in rare gas matrices and have not yet been detected directly in solution. Moreover, theoretical models based on C-H bond activation of methane support the position that the key reactive intermediate is a coordinatively-unsaturated species resulting from initial ligand photodissociation at the metal center.[10]

On the other hand, though, there is the possibility that associative reactions participate in these ligand-substitution and C-H bond activation processes.[11] Preliminary evidence was obtained for a ring slippage ($\eta^5 \rightarrow \eta^3$) mechanism in the matrix isolation studies of $(\eta^5\text{-}C_5R_5)M(CO)_2$ (M = Rh, Ir; R = H, Me) complexes[6a] but the interpretation of the results was subsequently presented in favor of the photoproduced unsaturated $(\eta^5\text{-}C_5R_5)M(CO)$ species again.[6b] The above conclusions, therefore, contrast with the known thermal chemistry in ligand substitutional processes of these types of molecules[12] which has implicated ring

(1) (a) Parshall, G. W. *Catalysis (London)* **1977**, *1*, 355. (b) Webster, D. E. *Adv. Organomet. Chem.* **1977**, *15*, 147. (c) Shilov, A. E.; Shteinman, A. A. *Coord. Chem. Rev.* **1977**, *24*, 97. (d) Parshall, G. W. *Homogeneous Catalysis*; Wiley-Interscience; New York, 1980. (e) Collman, J. P.; Hegedus, L. S. *Principles and Applications of Organotransition Metal Chemistry*; University Science Books: Mill Valley, CA, 1980.

(2) (a) Mills, O. S.; Nice, J. P. *J. Organomet. Chem.* **1967**, *10*, 337. (b) Oliver, A. J.; Graham, W. A. G. *Inorg. Chem.* **1971**, *10*, 1. (c) Hill, R.; Knox, S. A. R. *J. Chem. Soc., Dalton Trans.* **1975**, 2622. (d) Nutton, A.; Maitlis, P. M. *J. Organomet. Chem.* **1979**, *166*, C21.

(3) (a) Hoyano, J. K.; Graham, W. A. G. *J. Am. Chem. Soc.* **1982**, *104*, 3723. (b) Hoyano, J. K.; McMaster, A. D.; Graham, W. A. G. *J. Am. Chem. Soc.* **1983**, *105*, 7190.

(4) (a) Janowicz, A. H.; Bergman, R. G. *J. Am. Chem. Soc.* **1982**, *104*, 352; *J. Am. Chem. Soc.* **1983**, *105*, 3929. (b) Periana, R. A.; Bergman, R. G. *Organometallics* **1984**, *3*, 508. (c) Wax, M. J.; Stryker, J. M.; Buchanan, J. M.; Kovac, C. A.; Bergman, R. G. *J. Am. Chem. Soc.* **1984**, *106*, 1211. (d) Janowicz, A. H.; Periana, R. A.; Buchanan, J. M.; Kovak, C. A.; Stryker, J. M.; Wax, M. J.; Bergman, R. G. *Pure Appl. Chem.* **1984**, *56*, 13. (e) Periana, R. A.; Bergman, R. G. *J. Am. Chem. Soc.* **1984**, *106*, 7272.

(5) Jones, W. D.; Feher, F. J. *J. Am. Chem. Soc.* **1982**, *104*, 4240; *Organometallics* **1983**, *2*, 562, 686; *J. Am. Chem. Soc.* **1984**, *106*, 1650; *Inorg. Chem.* **1984**, *23*, 2376; *J. Am. Chem. Soc.* **1985**, *107*, 620.

(6) (a) Rest, A. J.; Whitwell, I.; Graham, W. A. G.; Hoyano, J. K.; McMaster, A. D. *J. Chem. Soc., Chem. Commun.* **1984**, 624; *J. Chem. Soc., Dalton Trans.* **1987**, 1181. (b) Bloyce, P. E.; Rest, A. J.; Whitwell, I.; Graham, W. A. G.; Holmes-Smith, R. *J. Chem. Soc., Chem. Commun.* **1988**, 846.

(7) (a) Haddleton, D. M. *J. Organomet. Chem.* **1986**, *311*, C21. (b) Haddleton, D. M.; Perutz, R. N. *J. Chem. Soc., Chem. Commun.* **1985**, 1372; *J. Chem. Soc., Chem. Commun.* **1986**, 1734. (c) Haddleton, D. M.; McCramley, A.; Perutz, R. N. *J. Am. Chem. Soc.* **1988**, *110*, 1810.

(8) (a) Belt, S. T.; Haddleton, D. M.; Perutz, R. N.; Smith, B. P. H.; Dixon, A. J. *J. Chem. Soc., Chem. Commun.* **1987**, 1347. (b) Belt, S. T.; Grevels, F.-W.; Koltzbücher, W. E.; McCamley, A.; Perutz, R. N. *J. Am. Chem. Soc.* **1989**, *111*, 8373.

(9) (a) Haddleton, D. M.; Perutz, R. N.; Jackson, S. A.; Upmacis, R. K.; Poliakoff, M. *J. Organomet. Chem.* **1986**, *311*, C15. (b) Sponsler, M. B.; Weiller, B. H.; Stoutland, P. O.; Bergman, R. G. *J. Am. Chem. Soc.* **1989**, *111*, 6841. (c) Weiller, B. H.; Wasserman, E. P.; Bergman, R. G.; Moore, C. B.; Pimentel, G. C. *J. Am. Chem. Soc.* **1989**, *111*, 8288.

(10) (a) Saillard, J.-Y.; Hoffman, R. *J. Am. Chem. Soc.* **1984**, *106*, 2006. (b) Ziegler, T.; Tschinke, V.; Fan, L.; Becke, A. D. *J. Am. Chem. Soc.* **1989**, *111*, 9177.

(11) Marx, D. E.; Lees, A. J. *Inorg. Chem.* **1988**, *27*, 1121.

(12) (a) Schuster-Woldan, H. G.; Basolo, F. *J. Am. Chem. Soc.* **1966**, *88*, 1657. (b) Cramer, R.; Seiwell, L. P. *J. Organomet. Chem.* **1975**, *92*, 245. (c) Rerek, M. E.; Basolo, F. *Organometallics* **1983**, *2*, 372; *J. Am. Chem. Soc.* **1984**, *106*, 5908. (d) Ji, L.; Rerek, M. E.; Basolo, F. *Organometallics* **1984**, *3*, 740. (e) Cheong, M.; Basolo, F. *Organometallics* **1988**, *7*, 2041.

0002-7863/92/1514-4186$03.00/0

slippage mechanisms.[13] Consequently, our interest in this system has been stimulated by the dichotomy that apparently exists between its thermal and photochemical reactivities.

Herein, we present the results of an extensive study of the photochemistry of $CpRh(CO)_2$ and $Cp^*Rh(CO)_2$ ($Cp = \eta^5\text{-}C_5H_5$; $Cp^* = \eta^5\text{-}C_5Me_5$) in hydrocarbon solutions containing various phosphine and phosphite ligands; this follows from our earlier observations on ligand photosubstitution.[14] The photoreactivity of $(\eta^5\text{-}C_5R_5)Rh(CO)_2$ has also been determined in triethylsilane solutions to make a comparison with Si–H bond activation processes. The photochemical reactions studied here are characterized in detail; photoproducts have been identified, excitation wavelength effects have been investigated, and quantum efficiencies for these photoprocesses are reported. The results obtained enable us to formulate mechanisms for both ligand photosubstitution and photochemical C–H/Si–H bond activation and to resolve the issue of the nature of the reactive primary photoproduct.

Experimental Section

Materials. Dicarbonylchlororhodium(I) dimer and dicarbonylpentamethylcyclopentadienylrhodium(I) were obtained in high purity (>99%) from Strem Chemicals, Inc. and used as received. Cyclopentadienylthallium was purchased from Aldrich Chemical Co. in high purity (97%) and used without further purification. Solvents used in syntheses were obtained as reagent grade from Fisher Scientific Co. and were dried over anhydrous calcium sulfate (Aldrich Chemical Co.) prior to use. Solvents used in the photochemical studies were of photrex grade (Baker Chemical Co.). Neutral alumina chromatographic adsorbant (80–200 mesh) was obtained from Fisher Chemical Co. The triphenylphosphine (PPh_3), tri-*n*-butylphosphine ($P(n\text{-}Bu)_3$), trimethylphosphine (PMe_3), triethylphosphine (PEt_3), triphenyl phosphite ($P(OPh)_3$), tri-*n*-butyl phosphite ($P(O\text{-}n\text{-}Bu)_3$), and trimethyl phosphite ($P(OMe)_3$) ligands were all purchased from Aldrich Chemical Co. in high purity (97–99%); the liquids were distilled prior to use. Triethylsilane (Et_3SiH) was obtained from Aldrich Chemical Co. in high purity (99%) and was refluxed over 5 Å molecular sieve (Fisher Scientific Co.) for 4 h and subsequently distilled under a nitrogen atmosphere immediately prior to use. Nitrogen gas used for solvent deoxygenation was purchased as high research grade (>99.99% purity) and was itself deoxygenated and dried by passage over calcium sulfate (W. A. Hammond Co.), phosphorus pentoxide (Aldrich Chemical Co.), and a pelletized copper catalyst (BASF R3-11, Chemical Dynamics Co.) according to a previously described procedure.[15] Carbon monoxide was obtained from the Linde Gas division of Union Carbide as CP grade (99.5% purity) and was further purified by passage through a 1-m tube (2-cm diameter) containing the above copper catalyst and then a 25-cm tube (4-cm diameter) containing a mixture of calcium sulfate and 5 Å molecular sieve.

Synthesis of $CpRh(CO)_2$. This compound was prepared using an analogous procedure to that reported for $CpM(CO)_2$ (M = Rh, Ir) by Fischer et al.[16] Dicarbonylchlororhodium(I) dimer (0.25 g, 0.64 mmol) was dissolved in deoxygenated hexanes (150 mL) and continually stirred in a dry round-bottomed flask under a nitrogen atmosphere. Cyclopentadienylthallium (1.75 g, 6.5 mmol) was then added and the solution was refluxed under the nitrogen environment for 48 h in the dark. Subsequently, the reaction mixture was cooled and filtered to yield a yellow solution, which was reduced by rotary evaporation and chromatographed on a 10-cm column (2-cm diameter) containing neutral alumina (80–200 mesh) using hexanes as eluent. The final product was collected following rotary evaporation and was obtained in a yield of 40–60%; the product was stable for several weeks if stored in the dark at 273 K. IR, $CpRh(CO)_2$ in decalin: ν(CO) 2046, 1982 cm^{-1} (lit. as a liquid, 2051, 1987 cm^{-1}).[16a] UV–vis, $CpRh(CO)_2$ in decalin: λ_{max} 286 nm (ϵ = 3820 L mol^{-1} cm^{-1}), 420 nm (sh).

Synthesis of $CpRh(CO)PR_3$. The complexes were prepared and isolated according to the procedure reported by Schuster-Woldan and Basolo[12a] with minor modifications. The following preparation of $CpRh(CO)PPh_3$ is representative of the series. A reaction mixture containing $CpRh(CO)_2$ (0.25 g, 1.1 mmol) and PPh_3 (0.28 g, 1.07 mmol) in hexanes (40 mL) was refluxed for 12 h under N_2 in the dark. Red crystals were obtained after the reaction solution was cooled and concentrated by removal of 10 mL of solvent. The product crystals were collected by suction filtration, washed repeatedly with hexanes, and dried at room temperature. Impurities of PPh_3 were removed by sublimation under vacuum. Subsequently, the compound was redissolved in toluene and chromatographed on a 10-cm column (2-cm diameter) containing neutral alumina (80–200 mesh) to yield a bright orange solution. The solvent was removed by rotary evaporation and the resultant orange-red solid was collected in 55% yield. IR, $CpRh(CO)PPh_3$ in *n*-pentane: ν(CO) 1953 cm^{-1} (lit. in Nujol, 1942 cm^{-1}).[12a] UV–vis $CpRh(CO)PPh_3$ in *n*-pentane: 455 nm (ϵ = 135 L mol^{-1} cm^{-1}). Anal. C, 62.9; H, 4.40; Rh, 22.5. Found: C, 63.3; H, 4.68; Rh, 22.1.

The other complexes were prepared and purified analogously, with minor changes noted below. $CpRh(CO)P(n\text{-}Bu)_3$ was synthesized following a 2-h reflux in hexanes and the product was obtained as a red-brown oil. IR, $CpRh(CO)P(n\text{-}Bu)_3$ in *n*-pentane: ν(CO) 1943 cm^{-1} (lit. in Nujol, 1940 cm^{-1}).[12a] UV–vis, $CpRh(CO)P(n\text{-}Bu)_3$ in *n*-pentane: 430 nm (sh). $CpRh(CO)PEt_3$ was prepared via a 2-h reflux in hexanes to yield a red-brown oil. IR, $CpRh(CO)PEt_3$ in *n*-pentane: ν(CO) 1944 cm^{-1}. UV–vis, $CpRh(CO)PEt_3$ in *n*-pentane: 430 nm (sh). $CpRh(CO)PMe_3$ was synthesized via a 2-h reflux in hexanes to yield a brown oil. IR, $CpRh(CO)PMe_3$ in *n*-pentane: ν(CO) 1947 cm^{-1}. UV–vis, $CpRh(CO)PMe_3$ in *n*-pentane: 440 nm (sh). $CpRh(CO)P(OPh)_3$ was prepared by heating reagent materials in hexanes at 50 °C for 15 h. The product was obtained as a dark purple oil. IR, $CpRh(CO)P(OPh)_3$ in *n*-pentane: ν(CO) 1987 cm^{-1}. UV–vis, $CpRh(CO)P(OPh)_3$ in *n*-pentane: 460 nm (sh). $CpRh(CO)P(O\text{-}n\text{-}Bu)_3$ was synthesized by heating reagent materials in hexanes at 50 °C for 15 h and the product was obtained as a red-brown oil. IR, $CpRh(CO)P(O\text{-}n\text{-}Bu)_3$ in *n*-pentane: ν(CO) 1959 cm^{-1}. UV–vis, $CpRh(CO)P(O\text{-}n\text{-}Bu)_3$ in *n*-pentane: 430 nm (sh). $CpRh(CO)P(OMe)_3$ was prepared by heating reagent materials in hexanes at 50 °C for 15 h. The product was obtained as a red oil. IR, $CpRh(CO)P(OMe)_3$ in *n*-pentane: ν(CO) 1966 cm^{-1} (lit. as liquid, 1969 cm^{-1}).[12a] UV–vis, $CpRh(CO)P(OMe)_3$: 435 nm (sh).

Synthesis of $Cp^*Rh(CO)PR_3$. These complexes were prepared using similar procedures to those described above for the Cp derivatives.[12a,17] $Cp^*Rh(CO)PPh_3$ was obtained following a 15-h reflux of $Cp^*Rh(CO)_2$ (0.088 g, 0.3 mmol) and PPh_3 (0.144 g, 0.55 mmol) in dry benzene (5 mL). The reaction was carried out under N_2 and in the dark. Volatile materials were subsequently removed to yield an oily product. To this was added *n*-pentane (5 mL) and the solution was filtered and then chromatographed on alumina. Following removal of solvent the product was obtained as a deep red oil. IR, $Cp^*Rh(CO)PPh_3$ in *n*-pentane: ν(CO) 1947 cm^{-1}. UV–vis, $Cp^*Rh(CO)PPh_3$ in *n*-pentane: 450 nm (sh). Anal. Calcd: C, 65.9; H, 5.72; Rh, 19.5. Found: C, 66.4; H, 5.93; Rh, 19.1. The other Cp^* compounds were synthesized and purified analogously to yield deep red oils in each case. IR, $Cp^*Rh(CO)P(n\text{-}Bu)_3$ in *n*-pentane: ν(CO) 1931 cm^{-1}. UV–vis, $Cp^*Rh(CO)P(n\text{-}Bu)_3$ in *n*-pentane: 430 nm (sh). IR, $Cp^*Rh(CO)PMe_3$ in *n*-pentane: ν(CO) 1933 cm^{-1}. UV–vis, $Cp^*Rh(CO)PMe_3$ in *n*-pentane: 430 nm (sh). IR, $Cp^*Rh(CO)P(OPh)_3$ in *n*-pentane: ν(CO) 1963 cm^{-1}. UV–vis, $Cp^*Rh(CO)P(OPh)_3$ in *n*-pentane: 445 nm (sh). IR, $Cp^*Rh(CO)P(O\text{-}n\text{-}Bu)_3$ in *n*-pentane: ν(CO) 1944 cm^{-1}. UV–vis, $Cp^*Rh(CO)P(O\text{-}n\text{-}Bu)_3$ in *n*-pentane: 450 nm (sh). IR, $Cp^*Rh(CO)P(OMe)_3$ in *n*-pentane: ν(CO) 1950 cm^{-1}. UV–vis, $Cp^*Rh(CO)P(OMe)_3$ in *n*-pentane: 440 (sh).

Elemental analyses (C, H) were performed on several representative $CpRh(CO)PR_3$ and $Cp^*Rh(CO)PR_3$ complexes and were satisfactory.

Synthesis of $CpRh(CO)(Et_3Si)H$ and $Cp^*Rh(CO)(Et_3Si)H$. These complexes were prepared by UV irradiation for 3 h with a 200-W medium-pressure Hg lamp of $CpRh(CO)_2$ or $Cp^*Rh(CO)_2$ (0.3 mmol) in a solution of excess Et_3SiH (2 mL) in deoxygenated *n*-pentane (10 mL). After irradiation the volatile components were removed and the product was then redissolved in toluene and chromatographed on alumina. Following removal of solvent the products were obtained as yellow oils. IR, $CpRh(CO)(Et_3Si)H$ in *n*-pentane: ν(CO) 2010 cm^{-1} (lit. in hexane, 2012 cm^{-1}).[7a] UV–vis, $CpRh(CO)(Et_3Si)H$ in *n*-pentane: 290 nm. ^1H NMR of $CpRh(CO)(Et_3Si)H$ at 360 MHz in $CDCl_3$: in agreement with the literature.[7a] IR, $Cp^*Rh(CO)(Et_3Si)H$ in *n*-pentane: ν(CO) 1994 cm^{-1}. UV–vis, $Cp^*Rh(CO)(Et_3Si)H$ in *n*-pentane: 330 nm. ^1H NMR of $Cp^*Rh(CO)(Et_3Si)H$ at 360 MHz in $CDCl_3$, δ (ppm): 14.1 (doublet, J(Rh–H) = 37.4 Hz, RhH), 0.44 (quartet, J = 8.0 Hz, CH_2CH_3), 0.86 (triplet, J = 8.1 Hz, CH_2CH_3), 1.60 (singlet, C_5Me_5).

The IR carbonyl stretches for all the above isolated products agree closely with those obtained from the photochemical measurements in dilute solution.

Equipment and Procedures. Electronic absorption spectra were recorded on a Hewlett-Packard Model 8450A diode-array spectrometer and stored on a Hewlett-Packard Model 82901M disk drive. Spectra were obtained from solutions held in regular 1-cm quartz cuvettes and the reported band maxima are considered accurate to ±2 nm. Infrared

(13) O'Connor, J. M.; Casey, C. P. *Chem. Rev.* **1987**, *87*, 307.
(14) Drolet, D. P.; Lees, A. J. *J. Am. Chem. Soc.* **1990**, *112*, 5878.
(15) Schadt, M. J.; Gresalfi, N. J.; Lees, A. J. *Inorg. Chem.* **1985**, *24*, 2942.
(16) (a) Fischer, E. O.; Bittler, K. *Z. Naturforsch. B* **1961**, *16*, 225. (b) Fischer, E. O.; Brenner, K. S. *Z. Naturforsch. B* **1962**, *17*, 774.
(17) Werner, H.; Klingert, B. *J. Organomet. Chem.* **1982**, *233*, 365.

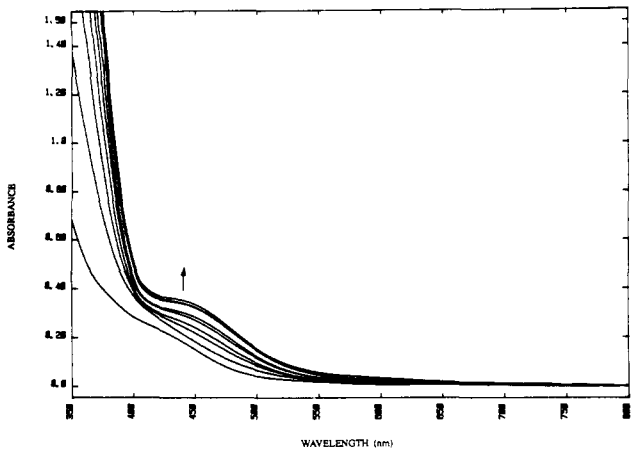

Figure 1. UV–visible absorption spectral changes accompanying the 458-nm photolysis of 2.5×10^{-3} M $CpRh(CO)_2$ in deoxygenated decalin solution containing 0.05 M PPh_3 at 283 K. Spectra are depicted following irradiation intervals of 1 h; initial spectrum recorded prior to irradiation.

spectra were recorded on a Nicolet Model 20SXC Fourier transform infrared (FTIR) spectrometer. Spectra were obtained from solutions using a NaCl cell of 1-mm path length and the reported band maxima are considered accurate to ± 0.5 cm^{-1}. FTIR spectra obtained from solid samples were recorded using a Barnes Spectra-Tech diffuse-reflectance attachment.

A Lexel Corp. Model 95-4 4 W argon-ion laser was used to perform the visible photolyses at 458 nm; the incident laser light intensity was determined by means of a Lexel Corp. Model 504 external power meter. Typically laser powers of 100–200 mW ($2.3–4.6 \times 10^{-5}$ einstein min^{-1}) were employed, although results were also obtained with reduced laser light powers of between 30 and 75 mW and the determined quantum efficiency values (see Results section) were not altered. Samples were irradiated with UV light from an Ealing Corp. medium-pressure 200-W mercury arc lamp and housing apparatus set on an optical rail; a 313-nm interference filter (Ealing Corp., 10-nm bandpass) was used to isolate the excitation wavelength. The incident light intensity at 313 nm was determined by ferrioxalate actinometry[18] and was typically in the range of $7.0–7.5 \times 10^{-7}$ einstein min^{-1}.

In all photolysis experiments the solution temperatures were controlled to ± 0.1 K between 268 and 293 K by circulating a thermostated ethylene glycol–water mixture through a jacketed cell holder mounted on the optical rail. Solutions were stringently filtered through 0.22-μm Millipore filters and deoxygenated by purging with prepurified nitrogen gas for 15 min prior to irradiation. Solutions saturated with CO were obtained by initially bubbling CO through the solution for 30 min and then stirring the solution for a further 30 min under a sealed CO atmosphere. During photolysis the solutions were rapidly stirred to ensure sample homogeneity and a uniform optical density in the light path. UV–visible and FTIR spectra were obtained from solutions at regular intervals throughout irradiation; resultant quantum efficiency values were determined in triplicate and were found to be reproducible to within $\pm 4\%$ in all cases. The stated uncertainties for the absolute quantum efficiency values incorporate systematic errors involved in measuring light intensity. Ligand substitution reactions were also performed in the dark to assess the extent of thermal processes and the reported quantum efficiency values are corrected for this contribution (typically 4–8% under our experimental conditions). Subsequent plots of quantum efficiency versus entering ligand concentration were fitted by standard least-squares linear regression analyses.

Results

Figure 1 illustrates the UV–visible absorption spectral changes accompanying the 458-nm photolysis of a deoxygenated decalin solution containing 2.5×10^{-3} M $CpRh(CO)_2$ and 0.05 M PPh_3 at 283 K. The spectra, acquired at irradiation time intervals of 1 h, reveal that the lowest absorption band of $CpRh(CO)_2$ appears as a shoulder centered at approximately 420 nm and that this

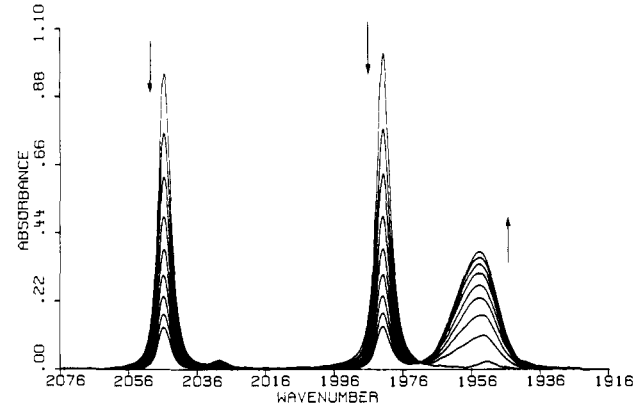

Figure 2. FTIR absorption spectral changes accompanying the 458-nm photolysis of 2.5×10^{-3} M $CpRh(CO)_2$ in deoxygenated decalin solution containing 0.05 M PPh_3 at 283 K. Spectra are depicted following irradiation time intervals of 1 h; initial spectrum recorded prior to irradiation.

feature is subject to a steady increase in the absorbance and a slight red shift during the course of the photochemical reaction. A substantial increase in absorbance at the exciting wavelength is also observed. Figure 2 depicts the FTIR spectral data recorded from the same photolysis experiment; the spectra indicate that there is a decline of the reactant's ν(CO) bands centered at 2046 and 1982 cm^{-1}, and the concurrent increase of a new feature at 1954 cm^{-1} representing the ν(CO) band of the $CpRh(CO)PPh_3$ photoproduct. The FTIR spectral results illustrate that there is a smooth photoconversion of reactant to product and that the reaction is uncomplicated by side or subsequent reactions, as evidenced by the absence of any other product bands in the FTIR spectral region and by the retention of sharp isosbestic points throughout the reactions. In addition, the $CpRh(CO)PPh_3$ complex is both thermally and photochemically stable under the conditions of the experiment. The fact that the reaction essentially involves stoichiometric conversion of the dicarbonyl complex to the monocarbonyl photoproduct (see eq 1) was confirmed by a

$$CpRh(CO)_2 \xrightarrow[PPh_3]{h\nu} CpRh(CO)PPh_3 + CO \qquad (1)$$

kinetic analysis of the FTIR spectra (vide infra) and the isolation of the $CpRh(CO)PPh_3$ complex (see Experimental Section). This photoreaction was not substantially affected by the competing analogous thermal process under our experimental conditions in the 268–293 K temperature range.

Similar ligand photosubstitution processes have been studied for $CpRh(CO)_2$ with a variety of entering phosphine and phosphite ligands (PR_3), and the FTIR spectral progressions obtained reveal that these reactions are also uncomplicated and result in stoichiometric conversion to the corresponding $CpRh(CO)PR_3$ photoproducts. These experiments were performed at 268 K to minimize the thermal contribution (typically 4–8%) from the competing thermal reactions. The $CpRh(CO)PR_3$ complexes were also isolated via thermal syntheses (see Experimental Section) to confirm the identity of these photoproducts.

Photoreactions of $CpRh(CO)_2$ were carried out in hydrocarbon solutions containing Et_3SiH to investigate the extent of Si–H bond activation and to make a comparison with the ligand photosubstitution processes. Figure 3 shows the UV–visible absorption spectral changes accompanying the 458-nm irradiation of a deoxygenated decalin solution containing 2.5×10^{-3} M $CpRh(CO)_2$ and 0.1 M Et_3SiH at 293 K. These spectra depict a steady decrease in the absorbance at the lowest energy band of $CpRh(CO)_2$ and at the excitation wavelength during the course of the photochemical reaction. Figure 4 illustrates the FTIR spectra obtained from the same photolysis experiment; the recorded spectra illustrate a decline in the absorbance of the reactant's ν(CO) bands at 2046 and 1982 cm^{-1} and the growth of a new band centered at 2009 cm^{-1} representing the ν(CO) mode of the $CpRh(CO)(Et_3Si)H$ photoproduct.[7a] The FTIR results again illustrate a clean progression during the formation of the photoproduct with the

(18) (a) Parker, C. A. *Proc. R. Soc. (London) A* **1953**, *220*, 104. (b) Hatchard, C. G.; Parker, C. A. *Proc. R. Soc. (London) A* **1956**, *235*, 518. (c) Calvert, J. G.; Pitts, J. N. *Photochemistry*; Wiley: New York, 1966.

(19) The concentration of CO in alkane solution at 283 K is approximately 9×10^{-3} M; see: Lawson, D. D. *Appl. Energy* **1980**, *6*, 241.

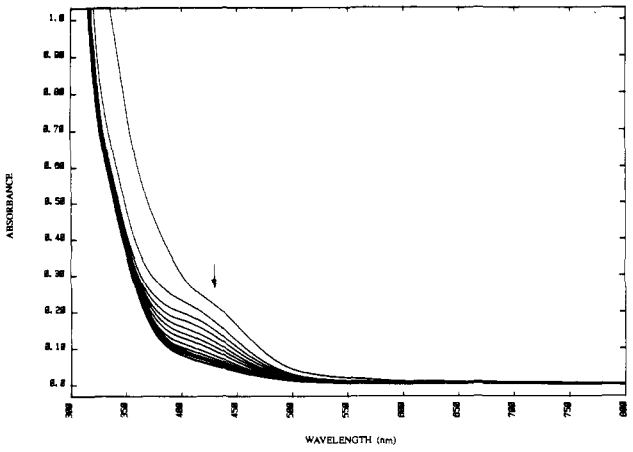

Figure 3. UV–visible absorption spectral changes accompanying the 458-nm photolysis of 2.5×10^{-3} M $CpRh(CO)_2$ in deoxygenated decalin solution containing 0.1 M Et_3SiH at 298 K. Spectra are depicted following irradiation time intervals of 30 min; initial spectrum recorded prior to irradiation.

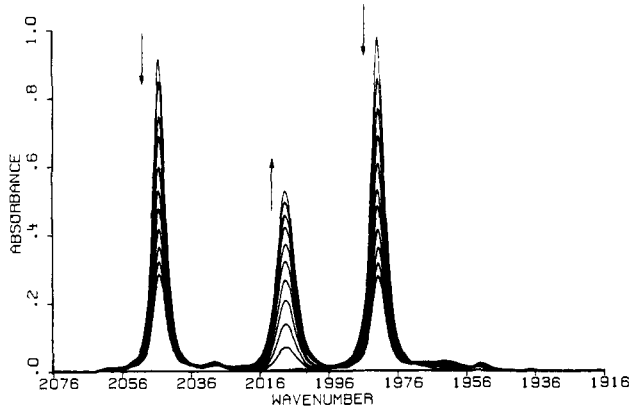

Figure 4. FTIR absorption spectral changes accompanying the 458-nm photolysis of 2.5×10^{-3} M $CpRh(CO)_2$ in deoxygenated decalin solution containing 0.1 M Et_3SiH at 298 K. Spectra are depicted following irradiation time intervals of 30 min; initial spectrum recorded prior to irradiation.

retention of sharp isosbestic points throughout the reaction. This photoreaction was also determined to result in a stoichiometric conversion to the hydrido product, according to eq 2, and to be essentially not influenced by any thermal contribution under the experimental conditions at 293 K. The $CpRh(CO)(Et_3Si)H$ photoproduct was isolated (see Experimental Section) to further confirm its nature.

$$CpRh(CO)_2 \xrightarrow[Et_3SiH]{h\nu} CpRh(CO)(Et_3Si)H + CO \qquad (2)$$

Ligand substitution and Si–H bond activation photoprocesses have also been investigated for the closely related $Cp^*Rh(CO)_2$ complex. The reactions are analogous to the processes described above (eqs 1 and 2), and they once again appear to be uncomplicated and result in near complete conversions to either the corresponding $Cp^*Rh(CO)PR_3$ or $Cp^*Rh(CO)(Et_3Si)H$ photoproducts. Typically these reactions were performed at 268 K because there was a negligible influence from any thermal reactions at this temperature. In all cases the $Cp^*Rh(CO)PR_3$ and $Cp^*Rh(CO)(Et_3Si)H$ complexes were isolated (see Experimental Section) to confirm the identity of these photoproducts.

Quantum efficiencies (ϕ_{cr}) have been determined for each of the above photoprocesses by application of eq 3. Here, C_R is the

$$-dC_R/dt = \phi_{cr}I_0(1 - 10^{-D})\epsilon_R b C_R/D \qquad (3)$$

concentration of the reactant complex at varying photolysis times t, I_0 is the incident light intensity per unit solution volume, b is the cell path length, D and ϵ_R are the optical density of the solution and molar absorptivity of the reactant complex at the irradiation wavelength, respectively, and ϕ_{cr} is the photochemical reaction quantum efficiency. It should be noted that D is the total optical density of the solution and it represents all the absorbing species; the factor $\epsilon_R b C_R/D$ is the fraction of the absorbed light that is absorbed by the reactant complex in the solution mixture.

Thus, eq 3 accounts for the inner filter effects caused by the increasing light absorption by the photoproduct during the reaction and, if necessary, any light absorption by the scavenging ligand. Rearrangement and integration of eq 3 yields eqs 4 and 5.

$$d \ln C_R = -\phi_{cr}I_0\epsilon_R b[(1 - 10^{-D})/D]\, dt \qquad (4)$$

$$\ln (C_{t_i}/C_{t_0}) = \alpha \int_{t_0}^{t_i} [(1 - 10^{-D})/D]\, dt \qquad (5)$$

where

$$\alpha = -\phi_{cr}I_0\epsilon_R b \qquad (6)$$

Plots of $\ln [(A_t - A_\infty)/(A_0 - A_\infty)]$ versus $\int_{t_0}^{t_i}[(1 - 10^{-D})/D]\, dt$, where A_0, A_t, and A_∞ are the FTIR absorbance values of the reactant's ν(CO) bands throughout photolysis, were observed to yield straight lines of slope α (units of reciprocal time) to reaction completion when $A_\infty = 0$, consistent with the observations from the FTIR spectra that the photoconversion of the reactant complex is clean and complete. Coincident α values were obtained on monitoring the declining absorbance of both ν(CO) bands of the reagent complex. Values of α were also obtained for the increasing absorbance reading of the ν(CO) band of the monocarbonyl photoproduct (here $\alpha = \phi_{cr}I_0\epsilon_R b$) and were identical, within experimental error, to the α values determined above, further confirming the stoichiometric nature of this photoreaction. Moreover, the resultant ϕ_{cr} values were found to be unaffected by variations in the incident laser light intensity (see Experimental Section), illustrating that solution inhomogeneity (resulting in a non-uniform optical density) is not a factor in these photolysis experiments.

Quantum efficiency values have been obtained for the 458-nm photosubstitution of $CpRh(CO)_2$ at 283 K (see eq 1) with various concentrations (0.05–0.3 M) of PPh_3; the results, illustrating a linear dependence of ϕ_{cr} on $[PPh_3]$, are shown in Figure 5a (slope = 2.5×10^{-2} M^{-1}, intercept = 1.8×10^{-3}). In sharp contrast, the ϕ_{cr} data for the 458-nm photochemical Si–H bond activation reaction of $CpRh(CO)_2$ at 293 K (eq 2) are independent of variations in Et_3SiH concentration over the same 0.05–0.3 M range; these results are also incorporated in Figure 5a (slope = 8.8×10^{-4} M^{-1}, intercept = 2.3×10^{-3}). Significantly, when photolyses were performed with 0.05 M PPh_3 solutions that had been saturated with CO,[19] there was no change in the observed UV–visible and FTIR spectral progressions or the measured quantum efficiency results from the $CpRh(CO)_2$ complex. Similar observations have been made from the analogous reactions of the $Cp^*Rh(CO)_2$ complex, and the quantum efficiency data obtained are represented in Figure 5b for both the PPh_3 substitution (slope = 1.4×10^{-3} M^{-1}, intercept = 1.2×10^{-4}) and Et_3SiH activation (slope = 1.8×10^{-4} M^{-1}, intercept = 1.0×10^{-4}) processes. It is notable that the ϕ_{cr} values are reduced by over an order of magnitude in the Cp^* system compared to the Cp one and that the dependence on $[PPh_3]$ is slightly lower. Also, it is noticeable that in both the $CpRh(CO)_2$ and $Cp^*Rh(CO)_2$ molecules the ϕ_{cr} values for photosubstitution and Si–H activation appear to extrapolate to a common intercept.

Quantum efficiency values for the 458-nm photosubstitution reaction of $CpRh(CO)_2$ with 0.05 M PPh_3 were determined at various temperatures; the obtained ϕ_{cr} values are 2.1×10^{-3} (268 K), 3.0×10^{-3} (273 K), 2.7×10^{-3} (278 K), 3.2×10^{-3} (283 K), 3.7×10^{-3} (288 K), and 4.1×10^{-3} (293 K). The least-squares line of an Arrhenius-type plot of $\ln \phi_{cr}$ versus $1/T$ yields an apparent activation energy, E_a, of 15.5 kJ mol^{-1}.

The photoreaction of $CpRh(CO)_2$ was studied in deoxygenated decalin solution in the absence of any entering ligand. The UV–visible spectra obtained from 458-nm photolysis of such solutions differed substantially from the previous results (see Figure 1) in

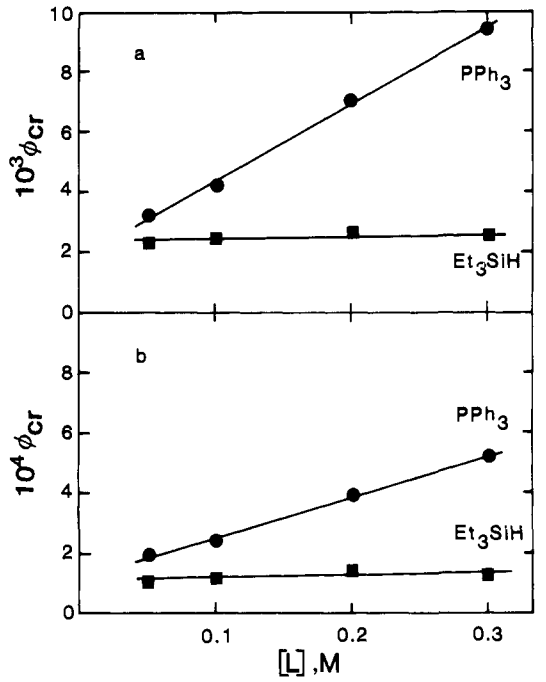

Figure 5. Plots of photochemical quantum efficiences (ϕ_{cr}) versus entering ligand (L) concentration for the reactions of (a) $CpRh(CO)_2$ and (b) $Cp^*Rh(CO)_2$ with PPh_3 and Et_3SiH. Excitation wavelength is 458 nm. Reaction with PPh_3 involves ligand substitution (eq 1) and reaction with Et_3SiH involves Si–H bond activation (eq 2). In (a) the photosubstitution data were obtained at 283 K and the Si–H bond activation data were recorded at 293 K. In (b) the data were obtained at 268 K. Each ϕ_{cr} value represents the mean of the least three readings; estimated uncertainties on ϕ_{cr} are within ±5%.

that a major larger absorbance increase was observed with the growth of new features at approximately 430 and 540 nm, characteristic of the red-colored carbonyl-bridged *trans*-$Cp_2Rh_2(CO)_3$ and purple-colored $[CpRh(\mu\text{-}CO)]_2$ complexes, respectively.[2c,8b] Additionally, FTIR spectra recorded from this reaction illustrate a steady decline in absorbance of the $\nu(CO)$ bands of the reactant $CpRh(CO)_2$ complex and appearance of new features centered at 1836 and 1778 cm^{-1}, confirming the formation of these CO-bridged photoproducts.[2c,8b] The photochemical reaction quantum efficiency for this process was measured over a 15% photoconversion and was determined to be 7.9×10^{-4}. Further photolysis of the reaction solution produced a dark red precipitate.

Photochemical quantum efficiencies at 458 nm have also been measured for ligand substitution of $CpRh(CO)_2$ with PMe_3 and $P(n\text{-}Bu)_3$ as a function of entering ligand concentration at 268 K. The results are shown in Figure 6a, revealing linear relationships of ϕ_{cr} with $[PR_3]$ in which the line slopes are also influenced by the nature of the scavenging ligand (PMe_3, slope = 0.10 M^{-1}, intercept = -1.2×10^{-4}; $P(n\text{-}Bu)_3$, slope = 4.7×10^{-2} M^{-1}, intercept = 8.4×10^{-4}). Quantum efficiencies have been determined for the 458-nm photosubstitution reactions of $CpRh(CO)_2$ and $Cp^*Rh(CO)_2$ complexes for a series of phosphine and phosphite ligands at 268 K. In all cases the FTIR spectra and the subsequent kinetic analysis reveal that the photosubstitution reaction takes place cleanly and is uncomplicated by any other secondary photochemical or thermal process. These measurements have all been performed at a constant entering ligand concentration of 0.05 M to minimize the thermal contribution; the results are listed in Table I and the reported ligand cone angle values[20] are included for comparison purposes. Measurements of ϕ_{cr} at higher $[PR_3]$ values were often hindered by the ligand solubility or by competing contributions from the accompanying thermal reaction.

(20) (a) Tolman, C. A. *J. Am. Chem. Soc.* **1970**, *92*, 2956. (b) Tolman, C. A. *Chem. Rev.* **1977**, *77*, 313.

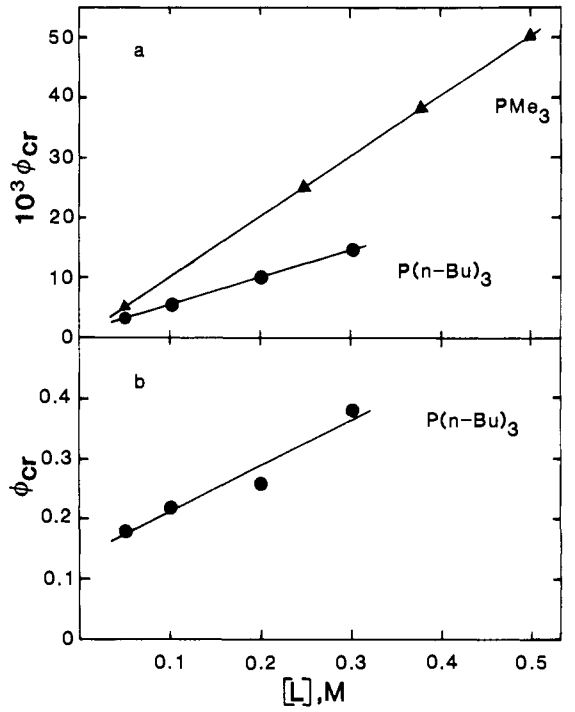

Figure 6. Plots of photochemical quantum efficiences (ϕ_{cr}) for the reaction of $CpRh(CO)_2$ with various concentrations of entering ligand, L = PMe_3 and $P(n\text{-}Bu)_3$, at 268 K. Excitation is at (a) 458 and (b) 313 nm. Each ϕ_{cr} value represents the mean of at least three readings; estimated uncertainties are within (a) ±5% and (b) ±10%.

Table I. Photosubstitution Quantum Efficiencies (ϕ_{cr}) for the 458-nm Conversion of $CpRh(CO)_2$ and $Cp^*Rh(CO)_2$ To Form the Corresponding CpRh(CO)L and Cp*Rh(CO)L Photoproducts in Deoxygenated Decalin at 268 K

		$10^3\phi_{cr}$[c]	
entering ligand[a]	ligand cone angle,[b] deg	Cp	Cp*
PPh_3	145	2.1	0.19
$P(n\text{-}Bu)_3$	132	3.1	0.21
PEt_3	132	4.3	0.24
PMe_3	118	5.2	0.32
$P(OPh)_3$	128	2.5	0.46
$P(O\text{-}n\text{-}Bu)_3$	112	6.3	0.21
$P(OMe)_3$	107	4.0	0.50

[a] Ligand concentration was 0.05 M for each reaction. [b] Values taken from ref 20. [c] Reported values are considered accurate to ±5%.

The photosubstitutional chemistry of $CpRh(CO)_2$ has been investigated following 313-nm excitation. For any particular entering ligand the UV–visible and FTIR spectra recorded from photolyses at 313 nm are identical in the types of spectral progression to those obtained on using 458-nm laser light (see Figures 1 and 2) and it is concluded that the same photoreaction takes place. Moreover, the spectral progressions are uncomplicated over greater than 50% of reaction conversion enabling quantum efficiencies to be calculated (see eqs 3–6). The ϕ_{cr} results for the 313-nm photolysis of 2.5×10^{-3} M $CpRh(CO)_2$ in deoxygenated decalin at 268 K containing various concentrations of $P(n\text{-}Bu)_3$ are depicted in Figure 6b (slope = 0.76 M^{-1}, intercept = 0.14). However, in comparing plots a and b in Figure 6 it is striking that the ϕ_{cr} values are increased by approximately two orders of magnitude in the experiments with the higher energy excitation wavelength (Figure 6b), although the latter ϕ_{cr} results are somewhat less influenced by the $P(n\text{-}Bu)_3$ concentration. Quantum efficiency results have also been determined for the 313-nm photosubstitution reactions of $CpRh(CO)_2$ with various phosphine and phosphite ligands; these are shown in Table II along with the reported ligand cone angle values.[20] All the 313-nm results were obtained with low entering ligand concentrations (0.05 M) and at a reduced temperature (268 K) to minimize the effects of interference from thermal processes.

Table II. Photosubstitution Quantum Efficiencies (ϕ_{cr}) for the 313-nm Conversion of $CpRh(CO)_2$ To Form the Corresponding $CpRh(CO)L$ Photoproducts in Deoxygenated Decalin at 268 K[a]

entering ligand	ligand cone angle,[b] deg	ϕ_{cr}[c]
$P(n\text{-}Bu)_3$	132	0.22
PEt_3	132	0.18
PMe_3	118	0.25
$P(O\text{-}n\text{-}Bu)_3$	112	0.16
$P(OMe)_3$	107	0.17

[a] Ligand concentration was 0.05 M for each reaction. [b] Values taken from ref 20. [c] Reported values are considered accurate to ±10%.

Discussion

General Comments on the Photochemistry. The observed photochemistry occurs following excitation into the lowest energy absorption bands of the $CpRh(CO)_2$ and $Cp^*Rh(CO)_2$ complexes. These transitions are thought to be ligand field (LF) in origin because the molar absorptivities of the electronic absorption bands are low. Moreover, the colors of the $CpM(CO)_2$ (M = Co, Rh, Ir) complexes in this series are red (Co), orange (Rh), and yellow (Ir), in accordance with the expected increases in LF strength associated with these metals.[21] In this connection, recent photophysical studies of $CpRh(CO)_2$ and $Cp^*Rh(CO)_2$ have revealed no luminescence from these materials as either solids or EPA glassy solutions at 77 K, implying that the lowest-energy excited states are short-lived.[22] This observation is consistent with a LF assignment.[23]

Ligand Photosubstitution. Two mechanistic pathways that may account for the experimental observations are shown below (eqs 7 and 8). Equation 7 represents a simple dissociative mechanism

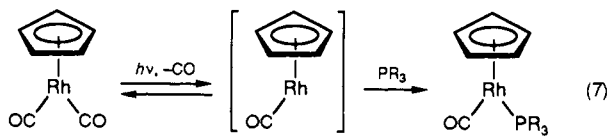

(7)

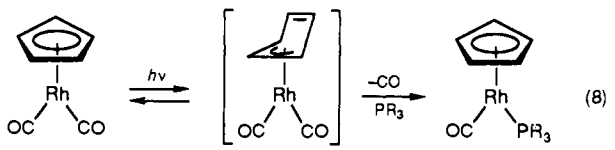

(8)

which involves the formation of a coordinatively-unsaturated 16-electron species as the primary photoproduct of the reaction; this intermediate is currently thought to be the reactive species in the photosubstitution and C–H bond activation processes.[6-10] In contrast, eq 8 describes a simple associative mechanism where the key reaction intermediate undergoes a $\eta^5 \rightarrow \eta^3$ ring slip and coordination of the incoming nucleophile. This mechanism is not presently recognized in the photoreactivity of these complexes, but it has been implicated in the corresponding thermal chemistry.[12,13]

Our photochemical quantum efficiency results cannot be rationalized by a simple dissociative-type mechanism (eq 7). This is because the ϕ_{cr} values obtained following both 458- and 313-nm excitations exhibit linear dependences on the entering ligand concentration (see Figures 5 and 6) and the lack of an observable effect on ϕ_{cr} with added CO. Taken together, these results illustrate that the primary photoproduct complex is not scavenged competitively by CO under the reaction conditions, while the ϕ_{cr} values are dependent on $[PR_3]$. This is not consistent with a dissociative mechanism whereby the PR_3 ligand, which is present in excess amounts, effectively scavenges all the photoproduced $CpRh(CO)$ species. Furthermore, the dependence of ϕ_{cr} on the nature of the phosphine or phosphite ligand (see Figures 5 and 6, Tables I and II) is not in accordance with a simple dissociative mechanism in which the entering ligand rapidly reacts with the coordinatively-unsaturated 16-electron intermediate. A kinetic scheme deriving the expected dependence of the quantum efficiency for photoproduct formation (ϕ_{prod}) for this mechanism is shown by eqs 9–16.

$$CpRh(CO)_2 \xrightarrow{I_{abs}} CpRh(CO) + CO \quad (9)$$

$$CpRh(CO) \xrightarrow[CO]{k_{-1}} CpRh(CO) \quad (10)$$

$$CpRh(CO) \xrightarrow[PR_3]{k_1} CpRh(CO)PR_3 \quad (11)$$

$$\frac{d[CpRh(CO)]}{dt} = I_{abs} - k_{-1}[CpRh(CO)][CO] - k_1[CpRh(CO)][PR_3] = 0 \quad (12)$$

$$[CpRh(CO)] = \frac{I_{abs}}{k_{-1}[CO] + k_1[PR_3]} \quad (13)$$

$$\frac{d[CpRh(CO)PR_3]}{dt} = \frac{k_1[PR_3]I_{abs}}{k_{-1}[CO] + k_1[PR_3]} \quad (14)$$

thus

$$\phi_{prod} = \frac{k_1[PR_3]}{k_{-1}[CO] + k_1[PR_3]} \quad (15)$$

and

$$\phi_{prod} = 1, \quad \text{if } k_1[CO] \ll k_1[PR_3] \quad (16)$$

It should be noted that ϕ_{prod} represents the quantum yield for photoproduct $CpRh(CO)PR_3$ generation in the absence of competing rate processes. The actual experimentally observed value of the reaction's photochemical quantum efficiency (ϕ_{cr}) thus incorporates other degradation mechanisms (such as radiative and nonradiative deactivation) that compete with bond dissociation from the reactive excited state. These photophysical aspects are further discussed below.

On the other hand, the photosubstitution results are entirely consistent with a simple associative-type mechanism. This is because the linear relationships of ϕ_{cr} on $[PR_3]$, and the dependence of ϕ_{cr} on the nature of PR_3, result from a bimolecular reaction in which the transition state involves coordination of the added nucleophile and, thus, the magnitude of the quantum efficiency is affected by the concentration and nature of the incoming ligand (see eqs 17–24 below). The lack of any influence of added CO on ϕ_{cr} is also predicted by a mechanism in which CO dissociation from the transition state is not rate limiting. Indeed, the ϕ_{cr} results obtained for all the phosphine and phosphite ligands (see Tables I and II) reveal a general trend with the entering ligand cone angle,[20] whereby ϕ_{cr} increases over the individual series of phosphines or phosphites as the ligand steric parameter reduces.[24] This relationship is more pronounced for the series of the phosphine ligands than the phosphite ligands, but it is noticeable for either the $CpRh(CO)_2$ or $Cp^*Rh(CO)_2$ systems. Additional factors that may affect the rate of the bimolecular reaction (and hence the ϕ_{cr} values) include the relative basicities of these ligands and the polarizability of the Rh–P bond formed following coordination[25]

$$CpRh(CO)_2 \xrightarrow{I_{abs}} (\eta^3\text{-}Cp)Rh(CO)_2 \quad (17)$$

$$(\eta^3\text{-}Cp)Rh(CO)_2 \xrightarrow{k_{-1}} CpRh(CO)_2 \quad (18)$$

$$(\eta^3\text{-}Cp)Rh(CO)_2 \xrightarrow[PR_3]{k_1} CpRh(CO)PR_3 + CO \quad (19)$$

(21) Geoffroy, G. L.; Wrighton, M. S. *Organometallic Photochemistry*; Academic Press: New York, 1979; p 155.
(22) Rawlins, K. A.; Lees, A. J.; Bloyce, P. E.; Rest, A. J., unpublished observations.
(23) Lees, A. J. *Chem. Rev.* **1987**, *87*, 711.
(24) (a) Halpern, J. *Pure Appl. Chem.* **1983**, *55*, 99. (b) Knowles, W. C. *Acc. Chem. Res.* **1983**, *16*, 106.
(25) (a) Streuli, C. A. *Anal. Chem.* **1959**, *31*, 1652; **1960**, *32*, 985. (b) Henderson, W. A.; Streuli, C. A. *J. Am. Chem. Soc.* **1960**, *82*, 5791. (d) Chalk, K. L.; Pomeroy, R. K. *Inorg. Chem.* **1984**, *23*, 444. (e) Boyles, M. L.; Brown, D. V.; Drake, D. A.; Hostetler, C. K.; Maves, C. K.; Mosbo, J. A. *Inorg. Chem.* **1985**, *24*, 3126.

$$\frac{d[(\eta^3\text{-Cp})Rh(CO)_2]}{dt} = I_{abs} - k_{-1}[(\eta^3\text{-Cp})Rh(CO)_2] - k_1[(\eta^3\text{-Cp})Rh(CO)_2][PR_3] = 0 \quad (20)$$

$$[(\eta^3\text{-Cp})Rh(CO)_2] = \frac{I_{abs}}{k_{-1} + k_1[PR_3]} \quad (21)$$

$$\frac{d[CpRh(CO)PR_3]}{dt} = \frac{k_1[PR_3]I_{abs}}{k_{-1} + k_1[PR_3]} \quad (22)$$

thus

$$\phi_{prod} = \frac{k_1[PR_3]}{k_{-1} + k_1[PR_3]} \quad (23)$$

and

$$\phi_{prod} = \frac{k_1[PR_3]}{k_{-1}}, \quad \text{if } k_{-1} \gg k_1[PR_3] \quad (24)$$

Again, for illustrative purposes ϕ_{prod} reflects the quantum efficiency of $CpRh(CO)PR_3$ formation in the absence of competing radiative and nonradiative deactivations from the reactive excited state. Consequently, ϕ_{prod} is predicted to exhibit linearity with $[PR_3]$, provided that the reaction quantum efficiencies are low; this behavior is indeed revealed by the experimental data plots (Figures 5 and 6a).

Further information about the reaction intermediate is obtained from the observed temperature dependence on ϕ_{cr} for the data involving PPh_3 substitution in $CpRh(CO)_2$. These results yielded an apparent activation energy of 15.5 kJ mol^{-1} which is relatively small and not atypical for thermal reactions of other transition-metal systems[26] and, in fact, it is similar to that obtained in the thermal studies performed on $CpRh(CO)_2$.[12] The low activation energy is not unreasonable for the replacement of solvent (S) by PR_3 in what is presumably a solvated $(\eta^3\text{-Cp})Rh(CO)_2\cdots S$ intermediate.[27]

Although a $\eta^5 \rightarrow \eta^3$ ring slip would appear to be the most likely explanation for the nature of the associative process, alternative hapticity changes such as a $\eta^5 \rightarrow \eta^1$ ring slip are also possible, or indeed other types of complex deformation (such as a bent $CpRh(CO)_2$ molecule) may enable the reaction to take place. While the ϕ_{cr} results clearly reveal an associative-type mechanism and this by implication is strongly suggestive of a $(\eta^3\text{-Cp})Rh(CO)_2PR_3$ species, they cannot be used to definitively assign a structure to the primary photoproduct. However, the quantum efficiency data for $Cp^*Rh(CO)_2$ do provide some important additional information in this connection. This is because the ϕ_{cr} results are strikingly reduced compared to the Cp system (see Figure 5 and Table I) and there is thus strong evidence that the ring is intrinsically involved in the photophysical mechanism that leads to the generation of the primary photoproduct. Both the photophysical characteristics of the molecule and the degree of steric hindrance about the ring will be affected on replacing the ring hydrogens of Cp with methyl groups to form Cp*. Each of these can be anticipated to influence the $\eta^5 \rightarrow \eta^3$ ring slippage process and the overall efficiency of the reaction via this route.[12,13,28,29] This aspect will be further discussed below. Importantly, an estimate of the lifetime of the transient species can also be obtained. Assuming that the reaction with the PR_3 nucleophile is diffusion controlled (i.e., estimating $k_{diff} = 1 \times 10^{10}$ L mol^{-1} s^{-1} and taking $[PR_3] = 0.05$ M), then this would place the lifetime of the primary photoproduct at 2×10^{-9} s. However, the actual lifetime may be somewhat shorter than this because of an extremely rapid $\eta^3 \rightarrow \eta^5$ back reaction; according to the above kinetic analysis (eqs 17–24), for the ϕ_{cr} plots to be linear then $k_{-1} \gg k_1[PR_3]$.

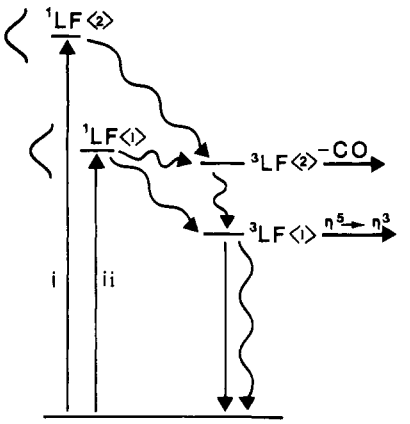

Figure 7. Photophysical representation of the low-energy excited states and their reactivities in $CpRh(CO)_2$ and $Cp^*Rh(CO)_2$ complexes following excitation at (i) 313 and (ii) 458 nm.

The photochemical results recorded with excitation at 313 nm confirm that the same photoreaction takes place and they also implicate an associative mechanism (see Figure 6). However, it is immediately noticeable on comparing the results in Tables I and II that ϕ_{cr} at 313 nm is substantially larger for any one of the phosphine or phosphite ligands than the ϕ_{cr} values obtained at 458 nm. This is a key result because the excitation wavelength dependence demonstrates unequivocally that a second and higher lying excited state is intrinsically involved in the photochemistry of these molecules. Moreover, the ϕ_{cr} values of Table II indicate that the ligand cone angle is considerably reduced upon higher energy excitation. These observations, taken together, clearly indicate that on excitation at 313 nm there is a significant contribution to the overall photoreaction from the population of a higher-lying excited state that more efficiently generates the $CpRh(CO)PR_3$ photoproduct via a dissociative pathway.

It should also be pointed out that there is some indication of nonlinearity from the ϕ_{cr} plot following 313-nm excitation (Figure 6b). As noted above eq 24 is only valid provided $\phi_{cr} \ll 1$ and so the ϕ_{cr} values should begin to show saturation at high ϕ_{cr} values as the excited states mainly form photoproducts. While the data of Figure 6b do indeed reveal more divergence from linearity, it would be necessary to investigate effects of ϕ_{cr} over a wider range of ligand concentrations to be able to draw any firm conclusions regarding a limiting effect. Finally, it is important to recognize that the intercepts of the ϕ_{cr} versus $[PR_3]$ plots are not zero following excitation with either the 313- or 458-nm wavelengths. This illustrates that there is an additional component to the mechanism that does not involve bimolecular processes with PR_3.

Photochemical Si–H Bond Activation. In sharp contrast to the photosubstitution results, the ϕ_{cr} data recorded in Et_3SiH solutions for both the $CpRh(CO)_2$ and $Cp^*Rh(CO)_2$ systems are not dependent on Et_3SiH concentration (see Figure 5). The following

(26) (a) Darensbourg, D. J.; Brown, T. L. *Inorg. Chem.* **1968**, *7*, 1679. (b) Ingemanson, C. M.; Angelici, R. J. *Inorg. Chem.* **1968**, *7*, 2646. (c) Covey, W. D.; Brown, T. L. *Inorg. Chem.* **1973**, *12*, 2820. (d) Darensbourg, D. J.; Ewen, J. A. *Inorg. Chem.* **1981**, *20*, 4168. (e) Drolet, D. P.; Chan, L.; Lees, A. J. *Organometallics* **1988**, *7*, 2502. (f) Moreno, C.; Macazaya, M. J.; Delgado, S. *Organometallics* **1991**, *10*, 1124.

(27) (a) Bonneau, R.; Kelly, J. M. *J. Am. Chem. Soc.* **1980**, *102*, 1220. (b) Lees, A. J.; Adamson, A. W. *Inorg. Chem.* **1981**, *20*, 4381. (c) Kelly, J. M.; Long, C.; Bonneau, R. *J. Phys. Chem.* **1983**, *87*, 3344. (d) Simon, J. D.; Xie, X. *J. Phys. Chem.* **1986**, *90*, 6751. (e) Simon, J. D.; Xie, X. *J. Phys. Chem.* **1986**, *90*, 6751; **1987**, *91*, 5538; **1989**, *93*, 291. (f) Wang, L.; Zhu, X.; Spears, K. G. *J. Am. Chem. Soc.* **1988**, *110*, 8695. (g) Joly, A. G.; Nelson, K. A. *J. Phys. Chem.* **1989**, *93*, 2876. (h) Lee, M.; Harris, C. B. *J. Am. Chem. Soc.* **1989**, *111*, 8963. (i) Xie, X.; Simon, J. D. *J. Am. Chem. Soc.* **1990**, *112*, 1130. (j) Yu, S.-C.; Xu, X.; Lingle, R.; Hopkins, J. B. *J. Am. Chem. Soc.* **1990**, *112*, 3668. (k) O'Driscoll, E.; Simon, J. D. *J. Am. Chem. Soc.* **1990**, *112*, 6580.

(28) King, R. B.; Bisnette, M. B. *J. Organomet. Chem.* **1967**, *8*, 287.

(29) (a) Cramer, R.; Seiwell, L. P. *J. Organomet. Chem.* **1975**, *92*, 245. (b) Bergman, R. G. *Acc. Chem. Res.* **1980**, *13*, 113. (d) Landon, S. J.; Brill, T. B. *J. Am. Chem. Soc.* **1982**, *104*, 6571. (c) Palmer, G. T.; Basolo, F.; Kool, L. B.; Rausch, M. D. *J. Am. Chem. Soc.* **1986**, *108*, 4417. (e) Freeman, J. W.; Basolo, F. *Organometallics* **1991**, *10*, 256.

Scheme I

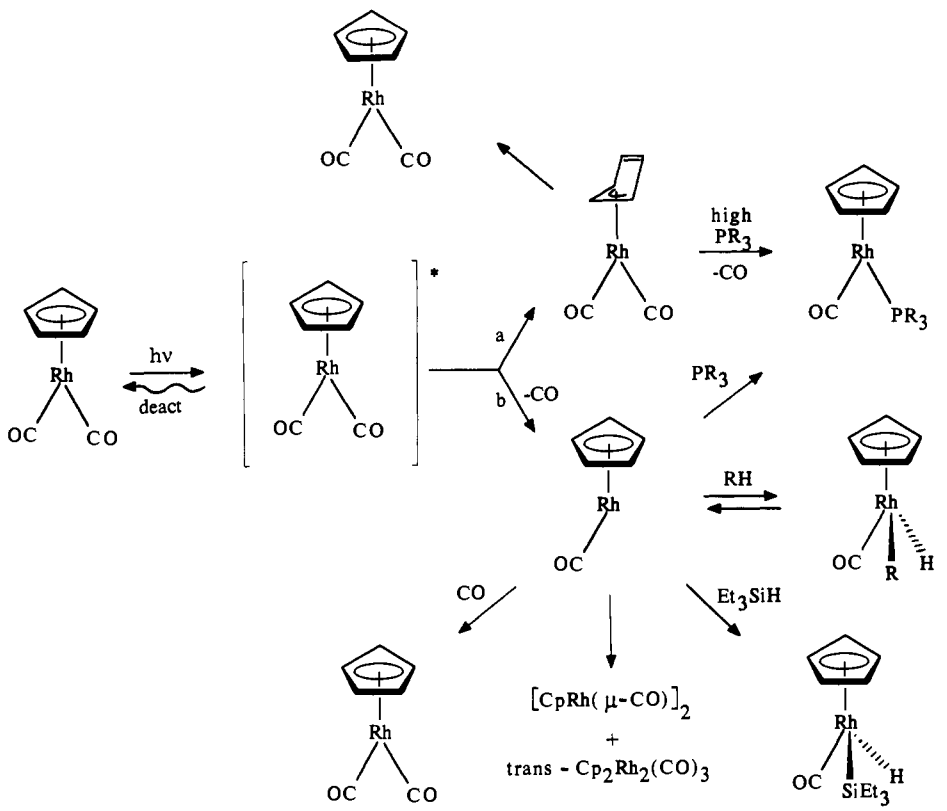

mechanistic pathway is postulated to account for these experimental observations (eq 25). Equation 25 represents a simple

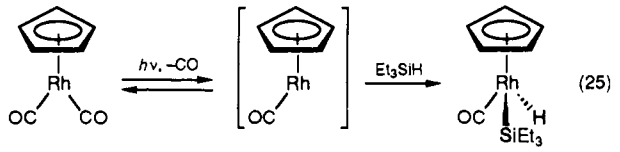

(25)

dissociative mechanism where the primary photoproduct is a coordinatively-unsaturated 16-electron species which is subsequently scavenged rapidly by the high concentration of Et_3SiH molecules. The independence of ϕ_{cr} on $[Et_3SiH]$ is entirely consistent with this simple dissociative pathway; the kinetic analysis is analogous to that presented above (see eqs 9–16), where Et_3SiH and $CpRh(CO)(Et_3Si)H$ replace PR_3 and $CpRh(CO)PR_3$, respectively. On the other hand, the observed photochemical results demonstrate unequivocally that the photochemical Si–H bond activation reaction does not proceed via an associative-type mechanism.

Solution Photochemistry: The Overall Reaction Scheme. Although the ligand substitution and Si–H bond activation mechanisms are seemingly so different, they can, in fact, be reconciled in an overall reaction pathway. Figure 7 and Scheme I portray the photophysical and photochemical routes that are believed to take place and which rationalize all of the experimental observations made in this study and in other work.[8b]

In Figure 7 the excitation wavelength dependence results are interpreted by recognizing that there is reaction from two different ligand field (LF) excited states. In this proposed photophysical representation absorption leads to ^{1}LF excited states which undergo rapid intersystem crossing to corresponding ^{3}LF levels.[30] On the basis of studies of the closely related group 6 metal hexacarbonyls, it is anticipated that these nonradiative processes are extremely fast (with a few picoseconds), as are the subsequent deactivation and bond dissociation events taking place from these electronically excited ^{3}LF states.[23,27] As noted above, the lack of an observable luminescence feature from these $CpRh(CO)_2$ and $Cp^*Rh(CO)_2$ complexes is consistent with the short-lived nature of the ^{3}LF levels. Thus, the photophysical processes are characterized both by efficient nonradiative deactivation from the excited ^{3}LF levels and by extremely rapid primary photoproduct formation. Under these conditions it is, therefore, reasonable to interpret the effects on ϕ_{cr} of varying the subsequent bimolecular processes (such as changing the nature or concentration of the scavenging ligand) in terms of the reactivity of the reaction intermediates that are produced.

The observation of two (associative and dissociative) reaction pathways from these $CpRh(CO)_2$ and $Cp^*Rh(CO)_2$ molecules indicates that the participating ^{3}LF levels produce primary photoproducts which have different reactivities. In accordance with the experimental data, the higher energy ^{3}LF state is designated to result in a CO dissociation reaction. Similarly, the lower energy ^{3}LF state is understood to result in a ring hapticity ($\eta^5 \rightarrow \eta^3$) change. It is important to realize, however, that the ϕ_{cr} data obtained reveal that both the $\eta^5 \rightarrow \eta^3$ and CO bond-breaking photoprocesses take place following excitation at either of the 313- or 458-nm irradiation wavelengths (vide infra). Accordingly, the CO dissociation process from the upper ^{3}LF excited state in the photophysical representation (Figure 7) must be competing with internal conversions to the lower ^{3}LF level and to the ground state. Furthermore, population of the ^{1}LF⟨1⟩ excited state upon 458-nm excitation must also lead to both the ^{3}LF⟨2⟩ and ^{3}LF⟨1⟩ levels via intersystem crossing mechanisms.[31]

It is a key feature of the mechanistic interpretation in Scheme I that a transient $(\eta^3\text{-Cp})CpRh(CO)_2$ complex is initially formed that is subsequently able to react directly with PR_3 (at high

(30) Designations of "pure" singlet and triplet excited states are precluded by the heavy metal center in these rhodium complexes (see ref 23 for further discussion).

(31) An alternative, albeit slightly more complicated, interpretation would involve intersystem crossing from the ^{1}LF⟨1⟩ and ^{1}LF⟨2⟩ levels to their respective ^{3}LF⟨1⟩ and ^{3}LF⟨2⟩ levels. The wavelength-dependent photochemistry could then be rationalized by having the ^{3}LF⟨2⟩ excited state undergo CO dissociation competitive with internal conversion to the ^{3}LF⟨1⟩ state and the ^{3}LF⟨1⟩ excited state able to undero **both** $\eta^5 \rightarrow \eta^3$ and CO dissociation processes.

concentrations of the scavenging nucleophile). As noted above, this molecule may be more accurately pictured as a solvated $(\eta^3\text{-Cp})Rh(CO)_2\cdots S$ species. Therefore, route a represents the associative component of the mechanism implicated by the ϕ_{cr} results for ligand photosubstitution (see eq 8); it results from the lowest lying $^3LF\langle 1\rangle$ excited state rapidly undergoing a $\eta^5 \rightarrow \eta^3$ ring slippage process and subsequent bimolecular reaction with the nucleophile at high PR_3 concentrations. This reaction will be in direct competition with the reverse ($\eta^3 \rightarrow \eta^5$) ring slippage process to regenerate the parent complex. Both the dependencies of the photochemical quantum efficiencies on $[PR_3]$ and the nature of PR_3 are thus explained by this description. Moreover, this process, while rate limited by $[PR_3]$, is unaffected by the addition of CO.

A second important feature of Scheme I is the competing formation of a higher energy ^3LF excited state which produces the intermediate CpRh(CO) by CO loss. Therefore, route b represents the dissociative component of the mechanism (see eqs 7 and 25). In the absence of nucleophiles (or at low nucleophile concentrations) the predominant reaction pathways are the secondary processes via this intermediate. The coordinatively-unsaturated 16-electron CpRh(CO) species is able to undergo Si–H or C–H bond activation reactions with Et_3SiH or RH, respectively, or alternatively it can react directly with PR_3 nucleophiles to form $CpRh(CO)PR_3$ or undergo a dimerization reaction to form $[CpRh(\mu\text{-CO})]_2$ and *trans*-$Cp_2Rh_2(CO)_3$.[8b] Our evidence for this dissociative process (route b) is the independence of ϕ_{cr} on $[Et_3SiH]$ and the nearly coincident intercepts on the ϕ_{cr} versus [L] plots for both the ligand substitution and Si–H bond activation reactions (see Figures 5 and 6a). In effect, the intercept of these plots represents the residual reaction occurring in the absence of either added nucleophile or Et_3SiH and it involves the generation of CpRh(CO)(R)H and the CO-bridged complexes. Again, the key intermediate here may be more accurately described as a solvated $CpRh(CO)\cdots S$ species.

The quantum efficiency results as a function of excitation wavelength can readily be interpreted with the aid of Scheme I. As we noted above in the photophysical representation (Figure 7), the measured ϕ_{cr} values at 313 nm reveal the increased participation of a dissociative component from a higher lying excited ^3LF state. Thus, excitation at the shorter wavelength (313 nm) substantially favors the CO dissociation pathway shown by route b; this rationalizes why the obtained ϕ_{cr} values themselves and the intercept of the ϕ_{cr} versus [L] plot are much greater (see Figure 6). On the other hand, the ϕ_{cr} results obtained upon 458-nm excitation imply that a greater proportion of lower lying $^3LF\langle 1\rangle$ excited states (see Figure 7) are formed, thereby favoring the ring slippage process. This conclusion is drawn because the efficiency of photoproduction of $CpRh(CO)PR_3$ is considerably reduced at 458 nm, which in turn implies that the $\eta^5 \rightarrow \eta^3$ pathway (route a) is enhanced compared to the dissociative pathway (route b). Under these conditions many molecules will undergo the $\eta^3 \rightarrow \eta^5$ back reaction. In this connection it is notable that recent results obtained from prolonged long wavelength (>400 nm) photolysis of $CpRh(CO)_2$ in solid CO also suggest that ring slippage products such as $(\eta^3\text{-Cp})Rh(CO)_3$ are formed in low yields.[32]

Scheme I equally explains the photochemistry of $Cp^*Rh(CO)_2$. It is interesting to note, however, that while the above observation of a virtually coincident intercept in plots of ϕ_{cr} versus [L] is also true for the Cp* system, the photoefficiency values at 458 nm are over an order of magnitude lower. Moreover, the slope of the linear relationship of ϕ_{cr} with $[PPh_3]$ is noticeably reduced for the $Cp^*Rh(CO)_2$ molecule (compare plots a and b in Figure 5). These aspects are enlightening because they demonstrate that the nature of the cyclopentadienyl ligand greatly influences the efficiency of the processes that lead to photoproducts and that both the associative and dissociative mechanisms are tempered in the Cp* system. Two reasons are offered that are in accordance with the photophysical processes (Figure 7) and mechanistic pathways (Scheme I). First, the efficiency at which the two reaction intermediates are formed is most likely to be reduced considerably due to the more effective nonradiative deactivation pathways expected from the ^3LF levels in Cp*; this is because the methyl-substituted cyclopentadienyl ligand introduces many more vibrational modes. Second, the back reaction of the key η^3-Cp reaction intermediate may be anticipated to be more efficient in the Cp* molecule than in the Cp system as the increased steric hindrance about the Cp* ring will effectively inhibit bimolecular reaction with PR_3 and tend to promote the $\eta^3 \rightarrow \eta^5$ back reaction.

Finally, it should be pointed out that the proposed scheme is entirely compatible with the flash photolysis results reported earlier describing these reactions arising from $CpRh(CO)$[8b] and the recent kinetic studies of $CpIr(CO)_2$ in liquefied noble gas solvents.[9] It is also not inconsistent with the quantum efficiencies determined in an earlier study of CpIr(CO) in perfluorobenzene (pfb)/benzene mixtures,[11] recognizing that pfb is reactive under those reaction conditions and forms a preequilibrium complex, CpIr(CO)(pfb), that itself absorbs light prior to C–H activating benzene.[33] Further effects aimed at identifying the $(\eta^3\text{-Cp})Rh(CO)_2\cdots S$ intermediate could involve time-resolved infrared (TRIR) spectroscopy of these systems or low-temperature studies in liquefied Xe in an attempt to stabilize a $(\eta^3\text{-Cp})Rh(CO)\cdots Xe$ complex. Alternatively, it may be possible to trap the $(\eta^3\text{-Cp})Rh(CO)_2$ species in weak nucleophilic solvents.

Conclusions

The experimental results have enabled us to describe an overall picture that portrays the photophysical deactivation and the ligand photosubstitution and photochemical C–H/Si–H bond activation processes for $CpRh(CO)_2$ and $Cp^*Rh(CO)_2$ in hydrocarbon solution. This reaction scheme involves photoprocesses from two different electronically excited states and it incorporates both associative and dissociative mechanisms. Moreover, it describes the nature of the reaction intermediates in both pathways. Importantly, it is demonstrated that ligand substitution takes place predominantly via bimolecular reaction of the entering nucleophile with a short-lived transient (a $\eta^5 \rightarrow \eta^3$ ring slipped species is implicated) and that intermolecular C–H/Si–H bond activations proceed via reactions directly with a coordinatively-unsaturated 16-electron intermediate.

Acknowledgment. We are grateful to the donors of the Petroleum Research Fund, administered by the American Chemical Society, and the Division of Chemical Sciences, Office of Basic Energy Sciences, Office of Energy Research, U.S. Department of Energy (Grant DE-FG02-89ER14039), for support of this research. Gratitude is extended to the Scientific Affairs Division of NATO for an International Collaboration Research Grant (0108/86) that has fascilitated a stimulating interaction with Dr. Derk J. Stufkens (University of Amsterdam). We are grateful to Agus A. Purwoko and Yi Han for experimental assistance. We also thank Professors Arthur W. Adamson (USC) and Robert G. Bergman (UC-Berkeley) for helpful discussions and Professor Robin N. Perutz (University of York) for useful comments and for providing results prior to publication.

(32) Perutz, R. N., private communication.

(33) (a) Drolet, D. P.; Lees, A. J., unpublished results. (b) Similar observations have been made following photolysis of $CpRh(PMe_3)(C_2H_4)$ and $Cp^*Rh(PMe_3)(C_2H_4)$ in pfb solutions and the corresponding $CpRh(PMe_3)(\eta^2\text{-}C_6F_6)$ and $Cp^*Rh(PMe_3)(\eta^2\text{-}C_6F_6)$ complexes have been isolated, see: Belt, S. T.; Duckett, S. B.; Helliwell, M.; Perutz, R. N. *J. Chem. Soc., Chem. Commun.* **1989**, 928. Jones, W. D.; Partridge, M. G.; Perutz, R. N. *J. Chem. Soc., Chem. Commun.* **1991**, 264.